SAE Aero Design East Competiton 2021 Design Report

FAMU-FSU College of Engineering
Team 057

Group Members:

Lauren Chin

Joseph Figari

Michenell Louis-Charles

Adrian Moya

Jacob Pifer

Sasindu Pinto

Cameron Riley

Noah Wright

STATEMENT OF COMPLIANCE
Certification of Qualification

Team Name	The Geese	Team Number	057
School	FAMU-FSU College of Engineering		
Faculty Advisor	Chiang Shih		
Faculty Advisor's Email	shih@eng.famu.fsu.edu		

Statement of Compliance

As faculty Adviser:

_____S_____ (Initial) I certify that the registered team members are enrolled in collegiate courses.

_____S_____ (Initial) I certify that this team has designed and constructed the radio-controlled aircraft in the past nine (9) months with the intention to use this aircraft in the **2021** SAE Aero Design competition, without direct assistance from professional engineers, R/C model experts, and/or related professionals.

_____S_____ (Initial) I certify that this year's Design Report has original content written by members of this year's team.

_____S_____ (Initial) I certify that all reused content have been properly referenced and is in compliance with the University's plagiarism and reuse policies.

_____S_____ (Initial) I certify that the team has used the Aero Design inspection checklist to inspect their aircraft before arrival at Technical Inspection and that the team will present this completed checklist, signed by the Faculty Advisor or Team Captain, to the inspectors before Technical Inspection begins.

Chiang Shih	1-22-2021
Signature of Faculty Advisor	Date
	1/22/2021
Signature of Team Captain	Date

Contents

List of Figures

List of Tables

Table 1: Symbols and Acronyms

Symbol	Description
L	Lift
D	Drag
AoA	Angle of attack
V	Velocity
C_L	Coefficient of lift
C_D	Coefficient of drag
C_M	Coefficient of moment
θ	Aileron deflection
δ	Rudder deflection
Θ	Elevator deflection

Acronym	Description
SAE	Society of Automotive Engineers
FAMU	Florida Agricultural and Mechanical University
FSU	Florida State University
RC	Radio Controlled
PLA	Polylactic Acid
CAD	Computer Aided Design
CFD	Computational Fluid Dynamics
CG	Center of Gravity
MAC	Mean Aerodynamic Chord
FBD	Free Body Diagram
NP	Neutral Point
MPH/mph	Miles per hour
LE	Leading Edge
TE	Trailing Edge

1 Executive Summary

The design report discusses the design and manufacturing process of the RC plane made for the SAE Aero Design Competition 2021 - East. We designed the plane to carry a size 5 soccer ball and a 1 *lb* cargo plate. Our plane weighs 12.3 lb without cargo and is 64.4 inches long. The team expects the plane to take off within 60 *ft*. To make our plane innovative, the team decided to use a canard wing as a secondary lift-producing wing, which is unusual for a cargo plane. We also decided to use woodworking techniques and geometric connection methods instead of mechanical fasteners to connect certain wing sections. Our cargo bay is between the canard and the main wing, closer to the CG of the plane, which is near the LE of the main wing. We primarily used SolidWorks, MATLAB, and xFoil for designing, and Cura for 3-D printing. Our goal is to show a different approach to creating and constructing RC cargo planes instead of using a conventional design and assembly. The following is the final design of the airplane.
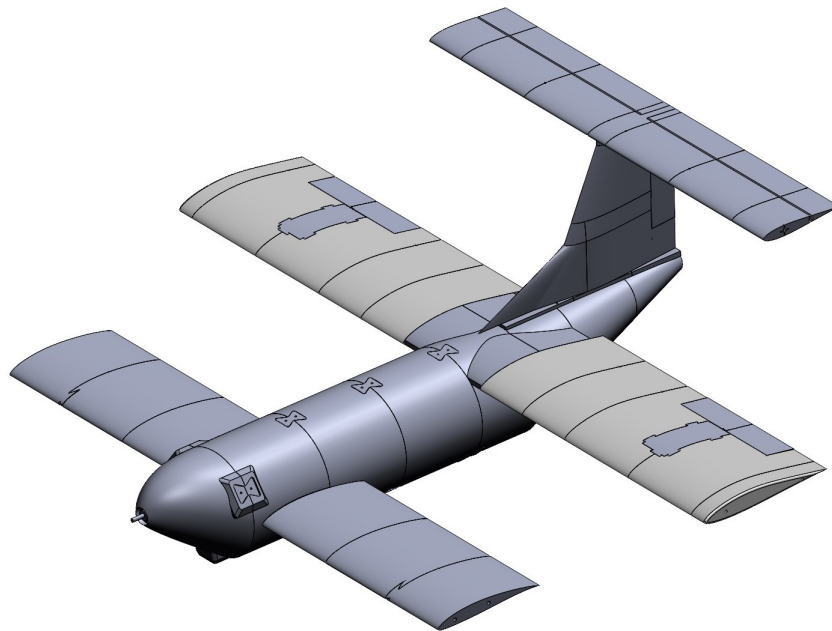

Figure 1: Final Design of the plane

2 Schedule Summary

We focused on research of different aircraft configurations and manufacturing processes in September and selected our concept in early December. While some team members were developing the CAD, others were focused on the electrical and mechanical components such as the motor circuit and control surface servo selection. Our main build material is slated to arrive by January 15th, following which we started printing the nose and fuselage. Assembly is slated to begin by the end of January, likely beginning with the fuselage and nose of the aircraft. Electronics installation and wing assembly will take place simultaneously. Assembly is expected to be finished by the third week of February.

Prelimiinary Research				Concept Generation						Concept Selection		
Aug 30- Sept 5	Sept 6-12	Sept 13 - 19	Sept 20-26	Sept 27- Oct 3	Oct 4-10	Oct 11- 17	Oct 18-24	Oct 25-31	Nov 1-7	Nov 8-14	Nov 18-21	Nov 22 -28
Sep-20					Oct-20				Nov-20			

Figure 2: Fall Design Schedule

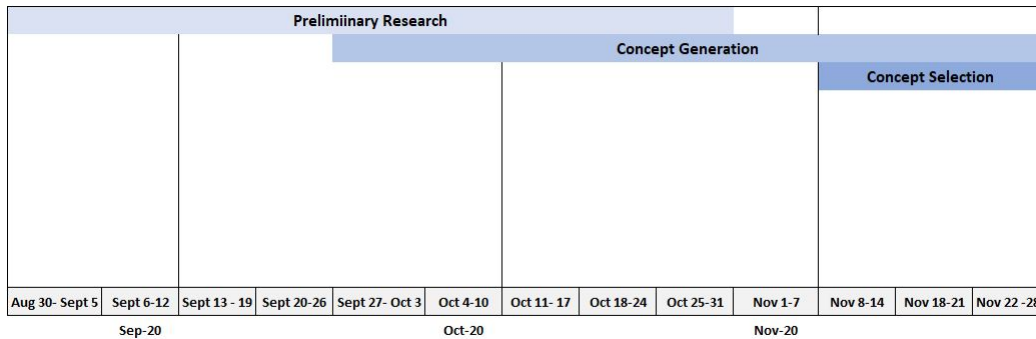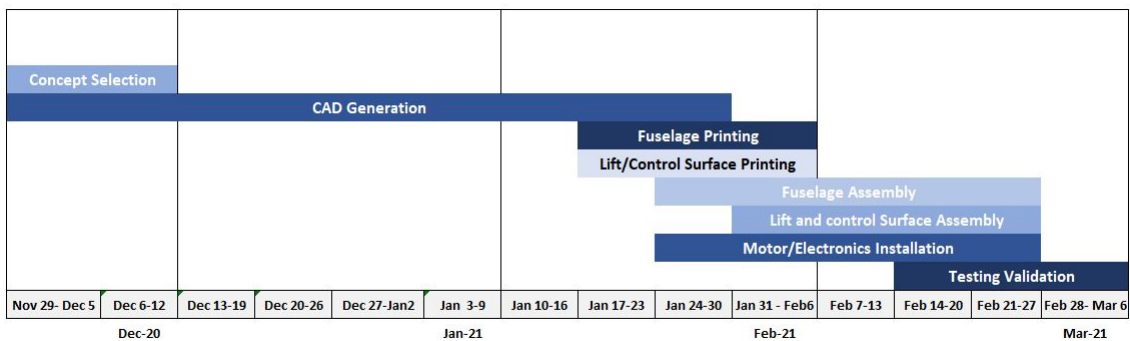|												
Concept Selection												
CAD Generation												
						Fuselage Printing						
						Lift/Control Surface Printing						
							Fuselage Assembly					
							Lift and control Surface Assembly					
							Motor/Electronics Installation					
										Testing Validation		
Nov 29- Dec 5	Dec 6-12	Dec 13-19	Dec 20-26	Dec 27-Jan2	Jan 3-9	Jan 10-16	Jan 17-23	Jan 24-30	Jan 31 - Feb6	Feb 7-13	Feb 14-20	Feb 21-27	Feb 28- Mar 6
Dec-20				Jan-21				Feb-21				Mar-21

Figure 3: Spring Design Schedule

3 Referenced Documents, References, and Specifications

Table 2: Table of References

Reference	Description
Airfoiltools.com. (2020). Retrieved November 2020, from: `http://airfoiltools.com/airfoil`	Purpose(s): C_M, C_L and C_D values for airfoil profiles Section(s): 4.3.2, 4.3.4, 6.2.1
Anderson, J.D. (2011). Fundamentals of Aerodynamics. 5th Edition New York, NY. The McGraw-Hill Companies, Inc.	Purpose(s): Lift and drag equations, static and dynamic stability Section(s): 5.1, 6.2.3, 6.2.4, 6.2.5, 6.2.6
ColorFabb: LW-PLA Natural. (2020). Retrieved October 2020, from: `https://colorfabb.com/lw-pla-natural`	Purpose(s): LW-PLA material properties Section(s): 6.3, 7, 8
Flite Test: How Ground Effect Vehicles Work. (2018) Retrieved January 2021, from `https://www.flitetest.com/articles/ground-effect`	Purpose(s): Ground effect information Section(s): 6.2.3
Lennon, A. (1999). Basics of RC model aircraft design: practical techniques for building better models. Ridgefiled, CT. Air Age Inc.	Purpose(s): Wing design research, control surface configuration research Section(s): 6.2.2, 6.2.5
Sadraey, M.H. (2013). Aircraft Design: A Systems Engineering Approach. 1st Edition. Nashua, NH. John Wiley and Suns Ltd.	Purpose(s) Control surface configuration research, lift and drag equations Section(s): 6.2.1, 6.2.2
The Engineering ToolBox: Air Properties. (2020). Retrieved December 2020, from `https://www.engineeringtoolbox.com/air-altitude-density-volume-d_195.html`	Purpose(s): Air pressure at different altitudes to calculate air density Section(s): 6.2.6

4 Design Layout Trades

4.1 Overall Design Layout and Size

Following research and calculations, we decided to use a canard - main wing - tail wing layout. Our team decided to install the canard as a mid wing to improve its effect on the CG, and the main wing as a high wing to reduce the effect of the wake from the canard. We decided to use a t-tail configuration for the tail section of the plane, as this would reduce the effect of the wake from the canard and the main wing on the horizontal section of the tail wing. While a bigger main wing would produce more lift, in have a canard layout, we needed the aspect ratio of the canard to be lower than the aspect ratio of the main wing. Lower aspect ratios result in a higher stall angle, which is what we desired with our canard. We decided to add ailerons to each main wing for roll control, a rudder to the horizontal part of the tail wing for yaw control, and an elevator that spans across the entire length of the horizontal part of the tail wing for pitch control. The Aileron span is 12.25 *in*, while the elevator and rudder spans are 47.5 *in* and 8 *in* respectively. Our propeller size is $18 \times 10E$.

4.2 Optimization

4.2.1 Optimization and Sensitivity Analysis

We decided to not taper the wings of our plane to maximize lift. This was possible as we have two lift producing wings, hence each one does not have to be very large. However, we decided to change the wingspans and the chord lengths to optimize the stability of our design and to fit our printer restrictions. We optimized the tail wing chord and wingspan to get the CG position to within 25% of the distance between the MAC of the canard and the main wing. Furthermore, we accounted the locations of the soccer ball and the 1 *lb* weight plate to ensure that the CG position will remain within the stability margin. For our design, the CG position had a margin of 2 *in* forward and 6 *in* backwards.

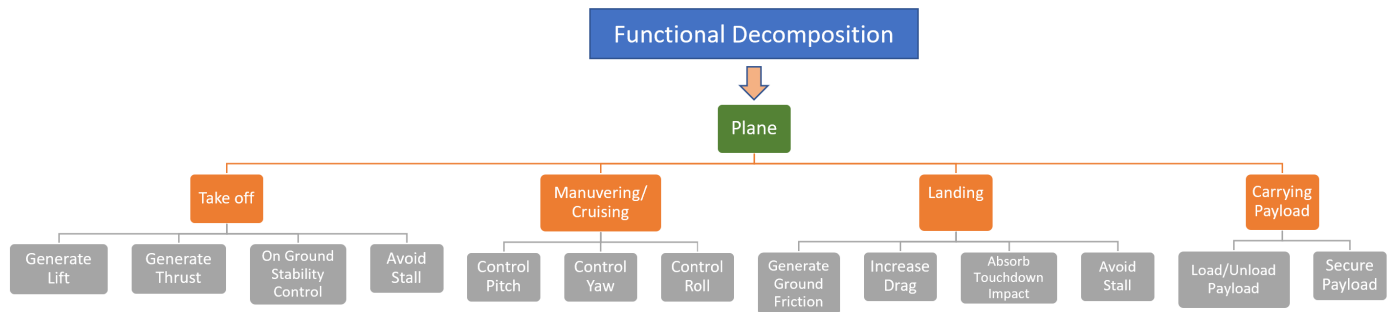## 4.3 Design Features and Details (Subassembly Sizing)

Figure 4: Functional Decomposition of the Project

We created the above functional decomposition to determine the systems we need to take into account in the design process.This was created following research on aircraft design and functionality. The major systems of our plane describe the key functions of our plane: takeoff, cruising, landing, and carrying a payload. The minor systems describe the actions our plane need to do to achieve major system functions. Based on these major and minor systems, we continued our design work.

4.3.1 Major Design Elements

With an eye for innovation, the team decided to add a canard to the plane. Our university's planes haven't taken off in previous years so the team went outside the box to create extra lift. The team decided to model the plane after the Rutan Quickie Q2. Through research it was found that our original design of the plane was unstable. To solve this issue a tail wing was added, which will be discussed further in the Stability Section (6.2.4)

4.3.2 Wing Layout

Our team's aircraft has three lift surfaces consisting of canards, a main wing, and a t-tail. The canards of our aircraft are straight and rectangular. We decided to add a canard to reduce the lift

load of the main wing and also to create a positive moment from the front of the plane during takeoff, which will reduce the workload of the elevator. The canards are strictly lift surfaces so they do not include any control surfaces. Furthermore, the addition of the canard reduced the wingspan of the main wing, which makes the wing less susceptible for flexing. The main wing of our aircraft is also straight and rectangular in shape. This lift surface will include ailerons to control rotation about the roll axis. After running preliminary stability calculations, a t-tail was included in our aircraft's design. The t-tail's purpose is to increase the stability of our aircraft and to re-position the center of gravity closer to the back of the aircraft. This reduces the wake on the horizontal section of the tail wing.
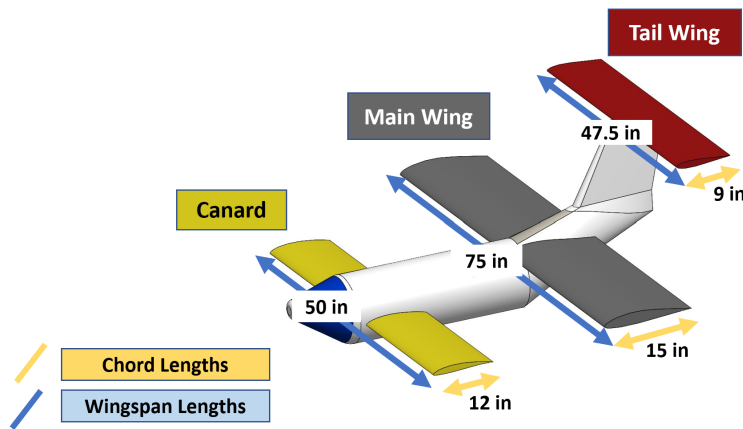
Figure 5: Plane Wing Dimensions

4.3.3 Cargo Hold

Due to the two wing layout, a top loading mechanism was designed. To do this a hatch was placed on top of the fuselage between the canards and the main wings. In putting it here, the cargo will placed at the plane's CG. This in turn will not make the plane unstable.

4.3.4 Airfoil Selection

Given the canard-main wing-tail wing layout, we decided to use asymmetric profiles for the canard and the main wing as they are predominant lifting wings, and a symmetric profile for the

tail wing as it is a stabilizer. We decided to use high lift profiles for the canard and the main wing to increase lift, while making sure that the canard has a lower stall angle of attack and a lower zero-lift angle of attack compared to the main wing. For the tail wing, we decided to use a profile with a high angle of attack as the tail wing is designed to stabilize the plane even when the canard and/or the main wing are near stall. We decided to use *Eppler E214* airfoil for the canard, *Eppler E197* airfoil for the main wing, and *Eppler 168* airfoil for the tail wing. Based on the C_L vs AoA Plot below (figure 6), our canard goes into stall before the main wing. Therefore, our airfoil profile selection is valid for our wing layout.
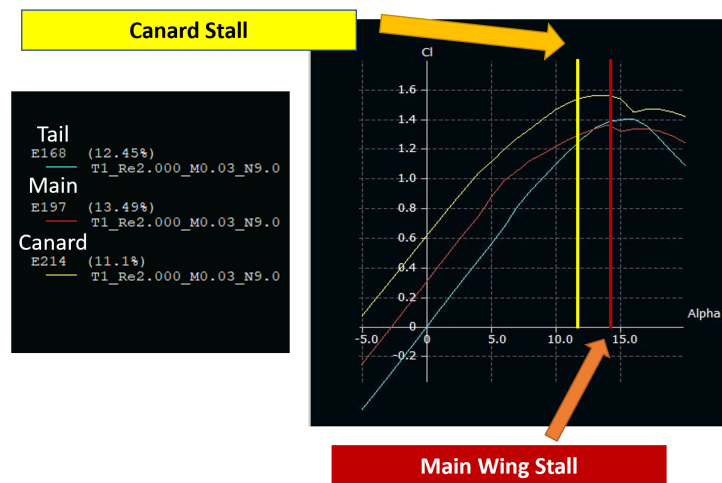

Figure 6: Xfoil Analysis of Airfoils: C_L vs AoA Plot

4.3.5 Propulsion System

The battery and motor were the two most important parts assessed for propulsion. The Onyx 22.2V 4000mAh 6S 30C LiPo Battery and E-flite 22.2V 5000mAh 6S 40C Thrust VSI LiPo Battery. These batteries have the same voltage, however the E-flite offers more current and a higher discharge rate. The Onyx is lighter, and was ultimately selected for financial reasons, as it is strong enough and was already owned by the college. Two motors were analyzed as well, the E-flite Power 90 Brushless Outrunner 325Kv and the E-flite Power 160 Brushless Outrunner 245Kv. Having the same manufacturer, the Power 160 is a stronger model, that comes with more weight at

a higher price. The team believed the Power 90 strong enough for our plane, and was selected for budget reasons as well, because it was already owned by the university. Before finalizing the components a thrust test was conducted with our equipment, as shown in figure 7.
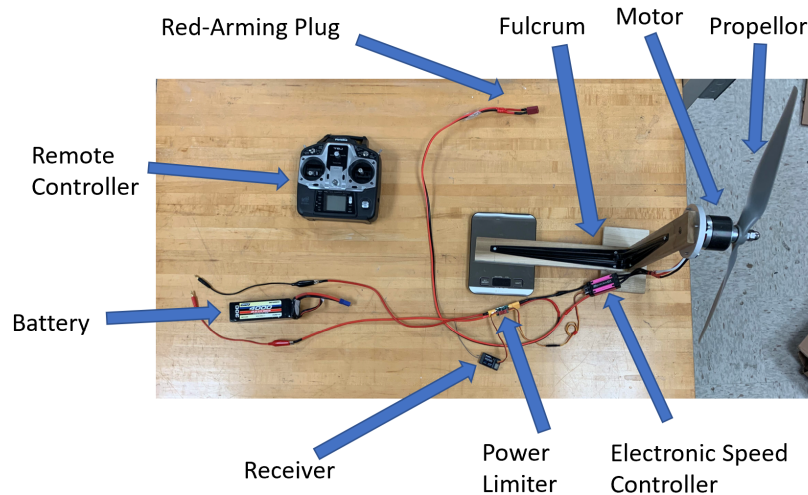

Figure 7: Thrust Test Setup

This setup features our motor, *an E-Flite Power-90*, attached to a fulcrum with two identical arms; one of the arms attached to the motor and the latter placed on a scale to measure the outputting thrust force. This was done to ensure that there was no mechanical advantage in play. Not shown in the figure but used in the setup were an electronic speed controller, a power limiter(limiting 1000 W to the motor as per the rule book), a receiver, and a red arming plug for safety. This setup was used to test a variety of different propellers to see which one generated the most thrust. Through this testing we found that the 18x10E propeller provided the most thrust at 222 lbf, which is higher than our necessary thrust calculated in section 5.2.3.

4.3.6   Landing Gear

We considered *tail-dragger* and *front tricycle* landing gear configurations. Through considering what is required at the competition, we selected the front tricycle configuration. Since the competition requires the plane to be steerable on the ground, having the single wheel at the front of the plane will make this easier for the operator. Having the single wheel ahead of the planes CG

also helps in keeping the plane from falling forward and breaking the propeller. The CG in this location helps correct the direction of the plane as well. If it is behind the single wheel, the inertia of the plane keeps it moving in the desired direction. We decided to distribute the weight 1:4 between the front and rear landing gears, as the rear landing gear is closer to the CG.

5   Loads and Environment Assumptions

5.1   Design Load Derivatives

Based on calculations, the team expect the plane to produce 31.4 *lbf* of drag. For our propeller, with the aforementioned drag, we expect an acceleration of 11.24 *ft/s* for our plane. We decided to use aluminum for our landing gears. With stall speed for our plane being 9.23 *mph*, with a safety factor of 1.3, our plane generates a total impact force of 465.84 *lbf*, with half of that applied to each rear landing gear, which We expect aluminum landing gears to withstand.

5.2   Environmental Considerations

We used typical cross-wind conditions expected in Lakeland,FL (9.6 *mph* average velocity) for yaw stability calculations during landing. However, given that the team does not expect to fly at a high altitude, air conditions considered for the majority of the calculations are standard air properties at sea level. Based on our thrust analysis, our plane can withstand a 10 mph headwind during takeoff. Therefore we expect our plane to withstand normal wind conditions in Lakeland.

6   Analysis

6.1   Analysis Technique

6.1.1   Analytical Tools

We decided to use MATLAB and Solidworks in conjunction for the analysis process, including the CFD tools in SolidWorks, and xFoil to evaluate lift and drag properties of the wings.

6.1.2   Developed Models

We used takeoff, flight maneuvering and landing models for the performance calculations done using MATLAB. The take off and landing model was analysed for standard sea level conditions, while maneuvering was done for equilibrium AoA of the plane at a 31.4 ft altitude.

6.2   Performance Analysis

6.2.1   Runway/Launch/Landing Performance

For our aircraft C_L/C_D value, which is considered the aerodynamic performance value for an aircraft, is maximum around 5° as shown in figure 8 below. Hence, we decided to use 5° as the takeoff angle of attack for our plane. For the maximum drag generated by the plane (31.4 lbf at 25 mph) we expect our plane to reach the desired 25 mph speed in 3.27 seconds, and 59.8 ft from the launch position. We have designed the plane to achieve its desired 5 ° AoA with 25 ° elevator deflection. The plane is expected to reach the desired flying altitude of 40 ft 12.48 seconds after launch. We included crosswind conditions expected in Lakeland, FL for landing analysis. Our plane takes 20.4 seconds to land, and travels 358.6 ft during approach. Once on the ground, we expect the plane to decelerate at 1.9 ft/s with just drag force, coming to a complete stop in 364.5 ft
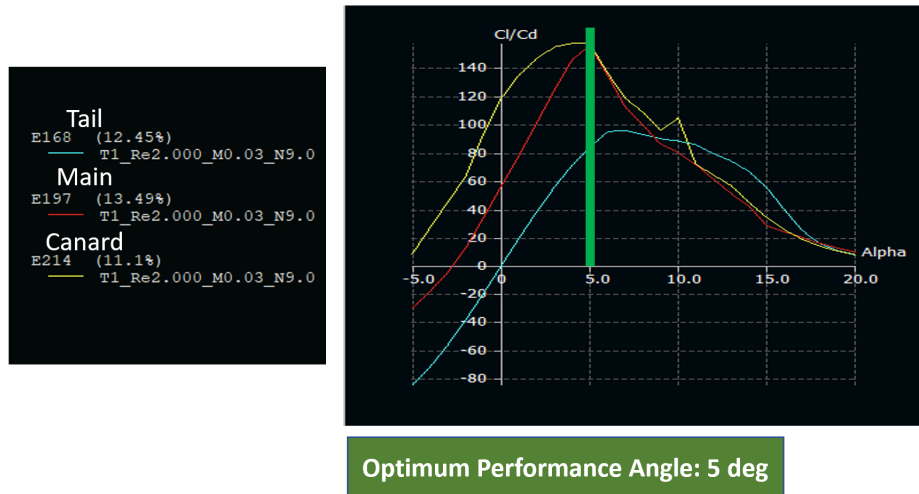
Figure 8: Xfoil Analysis of Airfoils: Aerodynamic Performance

.

6.2.2 Flight and Maneuver Performance

We will be using ailerons on each main wing while the rudder can be used to supplement aileron motion. We decided to use differential control for our ailerons, to avoid yaw instability in roll motion. We designed for 1:2.5 differential setting, with the maximum deflection angle (upwards) of an aileron been 20 °. The roll rate of our plane is 8.7 *deg/s*.

6.2.3 Shading/Downwash

In ground effect, during takeoff as the angle of attack increases the coefficient of lift increases; however, as the angle of attack increases the coefficient of drag increases as a squared effect. To avoid our airplane abruptly sinking to the runway once ground effect is left, we had to ensure that our airplane was producing enough thrust to maintain stable airspeed for climbing. Based on figure 9 below, our plane has relatively low vortices causing airflow disturbances. Therefore, we determined that clearance between our propeller and the ground is sufficient. We estimate our propeller to produce 222 *lbf* of static thrust through testing. The required thrust to reach our desired takeoff speed is 154 *lbf* of thrust; and the net thrust we are able to produce including drag

is 196 *lbf*. Based on these values, we concluded that there is sufficient thrust to escape ground effect using the reduced induced drag of the phenomena to our advantage.
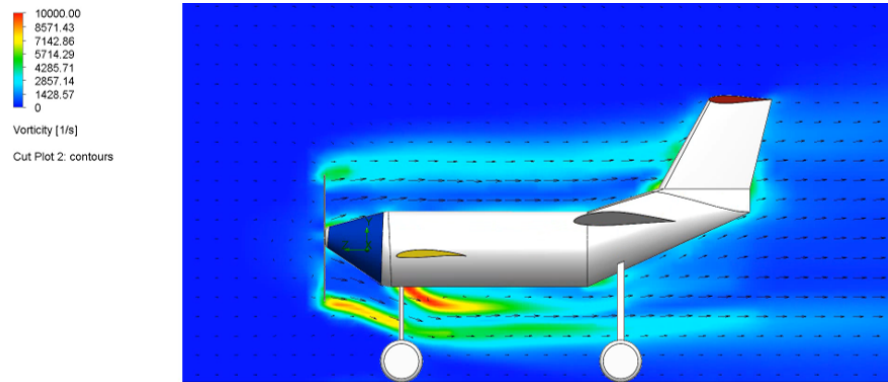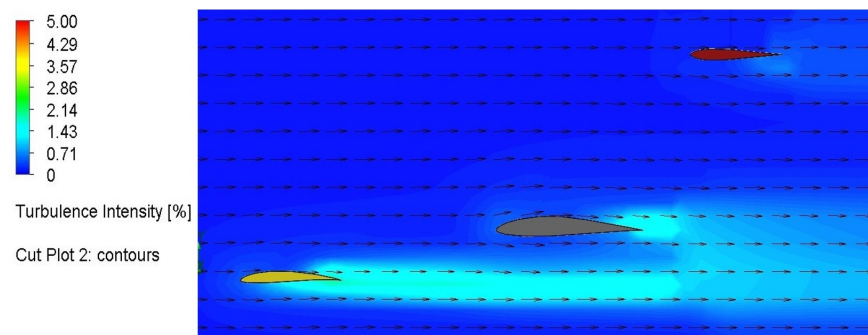

Figure 9: Ground Effects

Figure 10: Downwash effects on the wings

To further analyse downwash effects, we studied CFD across the wings as shown in figure 10. The turbulence for our design is relatively small, with a turbulence intensity of under 2%. Even at that intensity, downwash effect from the canard on the main wing is not significant as shown above. We decided to analyse the flow over the fuselage to determine the turbulence created by the fuselage. The main turbulence region is behind the plane as shown below. Furthermore, this validates the design consideration in placing the tail wing on the top of the vertical section of the tail, as downwash from the canard and the main wing is not effecting the horizontal tail wing.
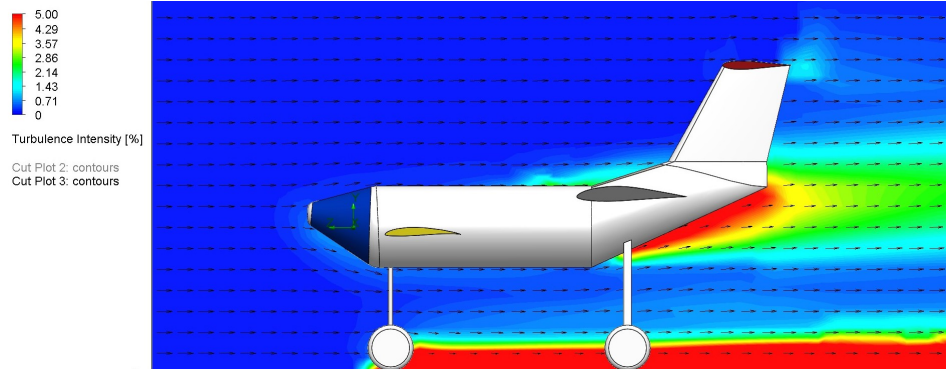
Figure 11: Turbulence from the fuselage

6.2.4 Dynamic and Static Stability

We calculated stability about the center of gravity (CG) of the plane. We decided to vary the battery location to get C_M vs AoA plot that has a positive trim and a negative gradient. Positive trim means that our plane will have a positive moment even when the AoA is zero. A negative gradient leads to a decrease in C_M, which means that the moment about CG of the plane will be zero at a positive AoA. We plotted C_M vs AoA initially for a canard-main wing layout without a tail wing. However, for the proportions and the design considered, we did not get a negative gradient for the plot. To get the desired value, we decided to add a tail wing for the plane. As the takeoff AoA was 5°, we desired a equilibrium angle of attack below that value. Following multiple adjustments to the tail wing and the battery location, we ended up with the following C_M vs AoA plot for our design. Based on the plot below, we get a positive moment coefficient of 0.17 at 0° AoA. Our equilibrium AoA is 3.125°. For differential ailerons discussed in section 6.2.2, our plane reach roll stability at 10 ° roll angle. We added a dorsal fin to improve yaw stability (discussed in 6.2.1). We calculated the neutral point (NP) of the plane at different angles of attack to ensure that the plane is stable, and NP for our design is behind the CG position before equilibrium AoA as desired.
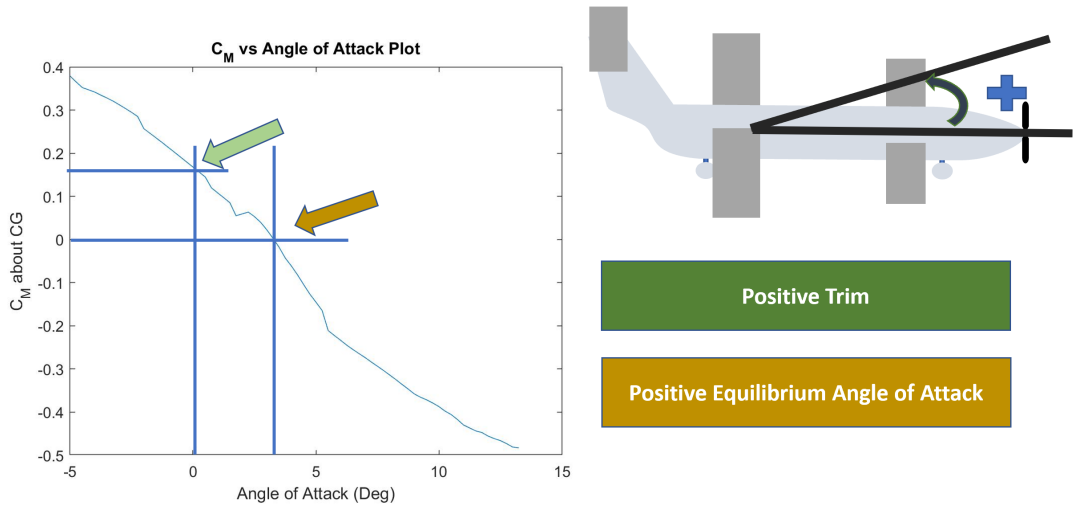
Figure 12: C_M vs AoA plot about CG

6.2.5 Aeroelasticity

As our plane is light weight, and that our maximum **Reynolds number is** 1.8×10^6, we expect large aerodynamic forces on our plane. Aerodynamic forces could cause the AoA of our plane to change, which is called divergence. We considered this in pitch stability calculations, which led to the addition of a tail wing and adjusting the dimensions of the canard and the main wing, Control surface movement cause a change in induced drag, which would cause a aerodynamic moment, creating a yaw instability. We considered this control reversal in setting the control surface deflection angles, which led to the 2.5:1 differential setting for our ailerons' deflection angles. Aerodynamic forces could cause vibrations on the plane, especially on the wings. We decided to include 2 spars going through the entire length on each wing to reduce this vibration effect, fluttering. Furthermore, this would reduce flexibility of the wings.

6.2.6 Lifting Performance, Payload Prediction, and Margin

We assumed that the lift generated by the fuselage is small relative to lift produced by the wings. We expect our plane to produce 15.9 *lbf* of lift at equilibrium (3.125° AoA) and 20.9 *lbf* of lift during take off (at 5° AoA). We predicted the payload for our plane using equilibrium AoA and air density

at different altitudes. Lift from all 3 wings were considered as the plane AoA is not zero. As lift is a function of dynamic pressure, which is a function of air density, we used this varying air density to get payload prediction at different altitudes. Accordingly, we plotted payload prediction for our plane (in Appendix B). We expect our plane to can carry a 13 lb weight at about 100 *ft*. Therefore, we expect our plane to fly with our 2 *lb* cargo load at the 40 ft altitude we plan on flying.

6.3 Structural Analysis

6.3.1 Applied Loads and Critical Margins Discussion
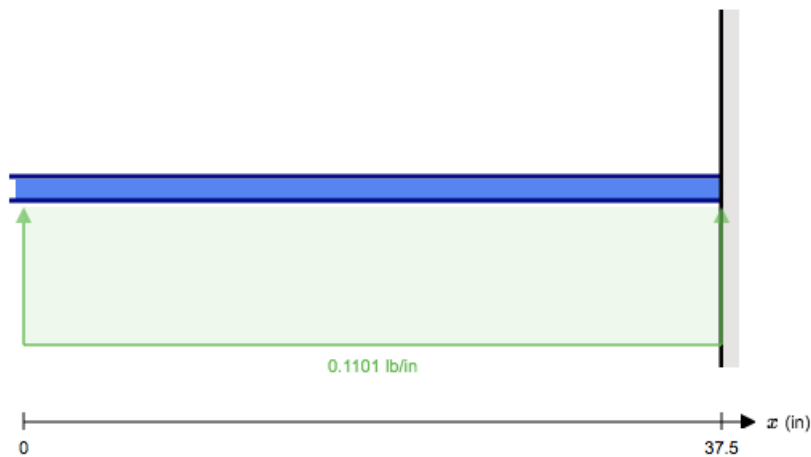

Figure 13: The set up for finding the moment and shear forces created by the main wing

When using additive manufacturing to build something that must endure some sort of load, the direction the parts are printed must be heavily considered. 3D printing can be thought of as layers of filament that are stacked on top of each other. With this being the case it can be very easy to break a part when a force is applied perpendicular to the printing direction. All that would need to happen for failure to occur would be two layers separating. Because of this the direction parts were printed in was heavily considered throughout the design of the plane. Arguably the most vulnerable parts of the plane are the wings. To test the forces each set of wings must endure, the wings were modeled as beams attached to a wall, with a distributed load under the beam as

shown in the force diagram above (figure 13). This was to simulate a single wing attached to the fuselage of the plane, with the distributed load (0.1101 *lb/in*)being the lift created by the wing. The setup for the main wings is shown above. Once the figures were created, the shear moment forces experienced at the connection point of the wing the fuselage were found.
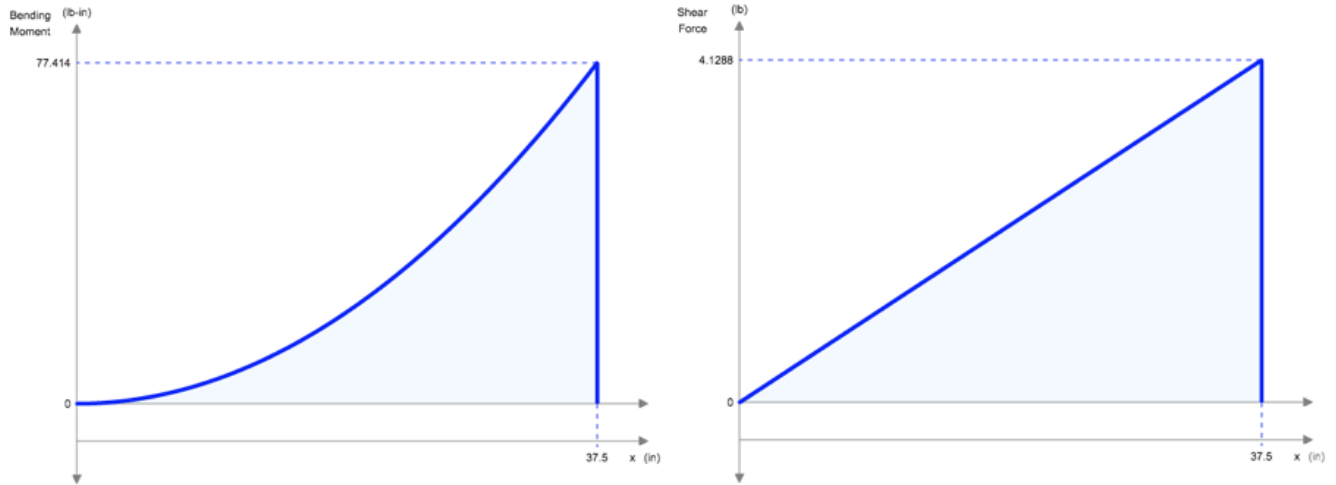

Figure 14: Moment and shear forces plane wings must endure

In the graphs, the x-axis is the length of the wing. 0 is the tip of the wing and 37.5 in the connection point at the fuselage. This calculation was made for each set of wings. The table below shows the magnitude of the forces each set will experience.

Table 3: Forces experienced by all wings

Wing:	Moment (lb x in):	Shear (lb):
Canard:	77.414	4.129
Main:	38.938	3.115
Tail:	19.178	1.615

A three point bending test and a torsion test were both done on samples of our printing filament. These were done since these are the two main stresses the plane will have to endure. The tests were done using samples printed at the same settings the plane parts will be printed at. The results of the tests are shown bellow. The stress direction refers to the direction the stress was applied with

21

respect to the printing direction of the sample.

Table 4: Material strength for forces applied in different directions

Stress Direction:	Shear Strength (psi):	Flexural Strength (psi):
Perpendicular	3,380	471
Parallel	6,120	552

As shown in the table, printing direction must be heavily considered. For easier assembly and more strength, the wings are also assembled using two 6061 Aluminum spars per wing set. With this being the case, the team is confident the wings will remain intact during flight.

6.3.2   Mass Properties and Balance

The weight of our plane without a cargo load is 10.8 *lbs.* and the CG position is 33 *in* from the leading edge of the nose and 3.3 *in* from the top of the fuselage. As the CG is just in front of the main wing, we expect the lift produced by the main wing of the plane to counter the majority of the weight of the plane, as desired during the planning stage.

7   Assembly and Subassembly, Test, and Integration
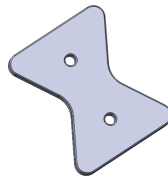
Figure 15: Bow tie used to connect pieces of the fuselage

Due to size constraints in 3D printing the plane, the aircraft was broken down into modular pieces. To connect pieces of the fuselage, small parts named bow ties were made to screw the parts together. The figure above shows one. To use the bow tie, screw threads had to be soldered into the parts of the fuselage being connected. A screw was then put through the holes of the bow tie and

screwed into the threads in the plane body. This added minimal weight to the plane and made it possible to assemble the fuselage. Each set of wings has 2 spars running from one tip to other other to increase rigidity of the wings as explained in section 6.3.1. Small crosses were also made to help lock the parts of the wings in place. These pieces again added minimal weight to the plane but helped in keeping the prints of the wing in place. This is shown in the exploded view below.

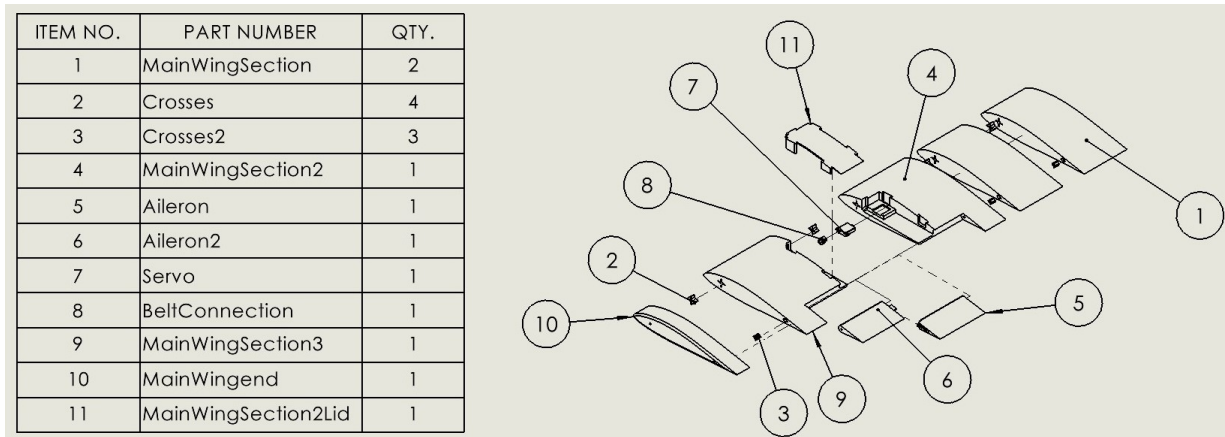| ITEM NO.	PART NUMBER	QTY.
1	MainWingSection	2
2	Crosses	4
3	Crosses2	3
4	MainWingSection2	1
5	Aileron	1
6	Aileron2	1
7	Servo	1
8	BeltConnection	1
9	MainWingSection3	1
10	MainWingend	1
11	MainWingSection2Lid	1

Figure 16: Exploded view of the main wing

The same assembly method was done for the canard and the tail. We divided the main wing into 5 pieces on each side, and we divided the canard into 3 pieces on each side. As the tail wing is on top of the tail section of the plane, we divided the entire tail wing into 7 pieces. For the canards, the final piece of the wing was connected using a dove tail joint. This is a common woodworking technique, and the team decided to explore the possibility of doing this in making RC planes. The figure below shows how the pieces connected.
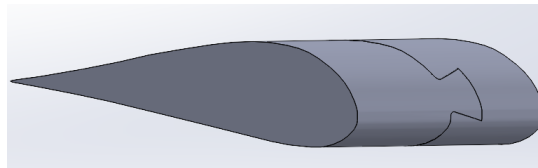

Figure 17: Woodworking technique used to connect the final pieces of the canards

The joint consists of a male female end on the parts. The male end is slid into place from the front of the wing. As the plane will only be moving forward during flight, this keeps the wing part

23

locked in place. This connection method was only used on the final piece to validate its usability.

8 Manufacturing

Using additive manufacturing to build an RC airplane is a nontraditional construction method. When doing so, a person must make sure the parts designed to assemble the plane are printable. Arguably the most important decision is what filament to use. The team considered PLA and light weight PLA (LW-PLA). PLA is a very common material used in additive manufacturing, as it is easy to use, relatively cheap, and prints accurately, but heavy. LW-PLA is a newer printing material made by the company colorFabb that foams when it leaves the printing nozzle, reducing the density and weight of the part. As we want a lighter plane, LW-PLA was chosen for printing. This material however can be difficult to print with. If the wrong printing settings are used warping can occur, resulting in a bad print. colorFabb has recommendations regarding things like printing temperatures and print speed to keep warping from happening. Between the company's recommendations and advice from last year's team, the plane's parts were printed at a temperature of 230°C and a speed of 30 mm/s. The Lulzbot printers used for this project were also placed in plastic containers to keep changes room temperature or humidity from affecting the prints as well. In doing so parts we were able to print accurately with the benefits of LW-PLA.

9 Conclusion

Following research on various designs and initial calculations, we decided to go with a canard-main wing-tail wing layout. The dimensions were adjusted to improve stability of the plane, while staying within the stability margin. Other than the addition of a canard, we decided to use wood-working techniques for assembly. We decided to include the cargo plane between the canard and the main wing to further improve stability. Overall, we believe that these design decisions have made our plane unique while producing a stable plane that can fly.

Appendix A - Backup Calculations

Contents

```
%All values in US units (in,lbf), unless otherwise specified
%References
%FOA - Fundamentals of Aerodynamics - John D. Anderson
%AD - Aircraft Design, A systems Engineering Approach - Mohhamad H. Sundraey
rho_ft=0.0023769;
rho=0.0023769/1728;    %slugs/ft3 / 1728 to get value in inches
```

Properties needed for calculatios

```
Weight_Plane=15; %12.316 % Max weight of the plane (rounded up to next whole number)
%Chord Lengths
Chord_canard=12; Chord_aft=14.5; Chord_tail=9;
%Wingspans
Wingspan_canard=50; Wingspan_aft=75; Wingspan_tail=47.5;

%Aspect Ratios (Reference - FOA)
AR_canard=Wingspan_canard^2/(Chord_canard*Wingspan_canard);
AR_aft=Wingspan_aft^2/(Chord_aft*Wingspan_aft);
AR_tail=Wingspan_tail^2/(Chord_tail*Wingspan_tail);
%Characteristic Length for Lift
S_canard=Chord_canard*Wingspan_canard;
S_aft=Chord_aft*Wingspan_aft;
S_tail=Chord_tail*Wingspan_tail;
%Characteristic Length for Lift in ft
S_canard_ft=Chord_canard*Wingspan_canard/144;
S_aft_ft=Chord_aft*Wingspan_aft/144;
S_tail_ft=Chord_tail*Wingspan_tail/144;

%Coefficient of Lift - AoA = 5 %deg, based on L/D plots
CL_canard=1.1174; CL_aft=0.8925; CL_tail=0.6417;
%Coefficient of Lift - AoA at 3.125 deg
CL_Eq_canard=0.93595; CL_Eq_aft=0.68385; CL_Eq_tail=0.34155;
%Coefficient of Lift - AoA at 3.125 deg
CD_Eq_canard=0.00675; CD_Eq_aft=0.00605; CD_Eq_tail=0.00785;
Thrust_From_test1=6.916*32.17 %Experimental Thrust for our propeller

%Velocity Conversions (Reference - FOA)
V_selected_in=25*17.6;    % selected 25 mph takeoff speed in in/s
V_selected_ft=25*1.467;   % takeoff speed in ft/s
q_selected=0.5*rho_ft*V_selected_ft^2; % corresponding dynamic pressure
% Reynolds # Calculations (Reference - FOA)
mu=3.734*10^(-7); %viscosity
Re_aft=(rho_ft*V_selected_ft*S_aft_ft)/(mu); %Re # for main wing
Re_canard=(rho_ft*V_selected_ft*S_canard_ft)/(mu) ; %Re # for canard
Re_tail=(rho_ft*V_selected_ft*S_tail_ft)/(mu) ; %Re # for tail wing
```

```
Thrust_From_test1 =

   222.4877
```

Drag Calculations (Reference - AD, FOA)

```matlab
%Skin Friction Drag
C_f_aft=0.074/(Re_aft^(1/5));   %skin friction drag coef. for aft
C_f_canard=0.074/(Re_canard^(1/5));   %skin friction drag coef. for canard
C_f_tail=0.074/(Re_tail^(1/5));   %skin friction drag coef. for canard
D_f=2*q_selected*C_f_aft*(S_aft) + 2*q_selected*C_f_canard*(S_canard) ...
    + 2*q_selected*C_f_tail*(S_tail); % skin friction drag

% Drag Calculations - Profile (Reference - FOA)
D_canard = CD_Eq_canard*q_selected*S_canard_ft; %Canard drag
D_aft = CD_Eq_aft*q_selected*S_aft_ft; %Main wing drag
D_tail = CD_Eq_tail*q_selected*S_tail_ft; %Tail wing drag

% Induced Drag (Reference - AD) (Reference - FOA)
e_lowmid=0.6;   %low/mid wing efficiency
e_high=0.8;     %high wing efficiency
%canard induced drag coefficient
Cd_i_canard=CL_Eq_canard^2/(pi*e_lowmid*AR_canard);
%main wing induced drag coefficient
Cd_i_aft=CL_Eq_aft^2/(pi*e_high*AR_aft);
%tail wing induced drag coefficient
Cd_i_tail=CL_Eq_tail^2/(pi*e_high*AR_tail);
D_i_canard=Cd_i_canard*q_selected*S_canard_ft; %canard induced drag
D_i_aft=Cd_i_aft*q_selected*S_aft_ft; %main wing induced drag
D_i_tail=Cd_i_tail*q_selected*S_tail_ft; %tail wing induced drag

%Total drag of the plane
D_Total= D_f + D_canard + D_aft + D_tail + D_i_aft + D_i_canard +D_i_tail
```

```
D_Total =

   31.7401
```

Lift Calculations (Reference - FOA)

```matlab
%Equilibrium
%Lift produced by each wing at equilibrium
L_canard=CL_Eq_canard*q_selected*S_canard_ft;
L_aft=CL_Eq_aft*q_selected*S_aft_ft;
L_tail=CL_Eq_tail*q_selected*S_tail_ft;
L_total_Eq=L_canard+L_aft+L_tail   %Total Lift

%Takeoff
%Lift produced by each wing at equilibrium
L_canard_to=CL_canard*q_selected*S_canard_ft;
```

```
L_aft_to=CL_aft*q_selected*S_aft_ft;
L_tail_to=CL_tail*q_selected*S_tail_ft;
L_total_to=L_canard_to+L_aft_to+L_tail_to    %Total Lift
thrust_net=Thrust_From_test1-D_Total
```

```
L_total_Eq =

    16.1104


L_total_to =

    21.2622


thrust_net =

   190.7476
```

Properties at takeoff (Reference - FOA)

```
%Acceleration
acceleration_to = (Thrust_From_test1-D_Total)/(Weight_Plane)
%time to get to 25 mph
time_req_acc = V_selected_ft/acceleration_to
%distance travelled
distance_travelled = V_selected_ft^2/(2*acceleration_to)
```

```
acceleration_to =

    12.7165


time_req_acc =

     2.8840


distance_travelled =

    52.8862
```

A-3

Appendix B - Technical Data Sheet

Team Name: The Geese   Team Number: 057

School: FAMU-FSU College of Engineering

The following is the payload prediction plot we generated. Steps we had taken to generate the plot and its outcomes are discussed in section 5.2.6
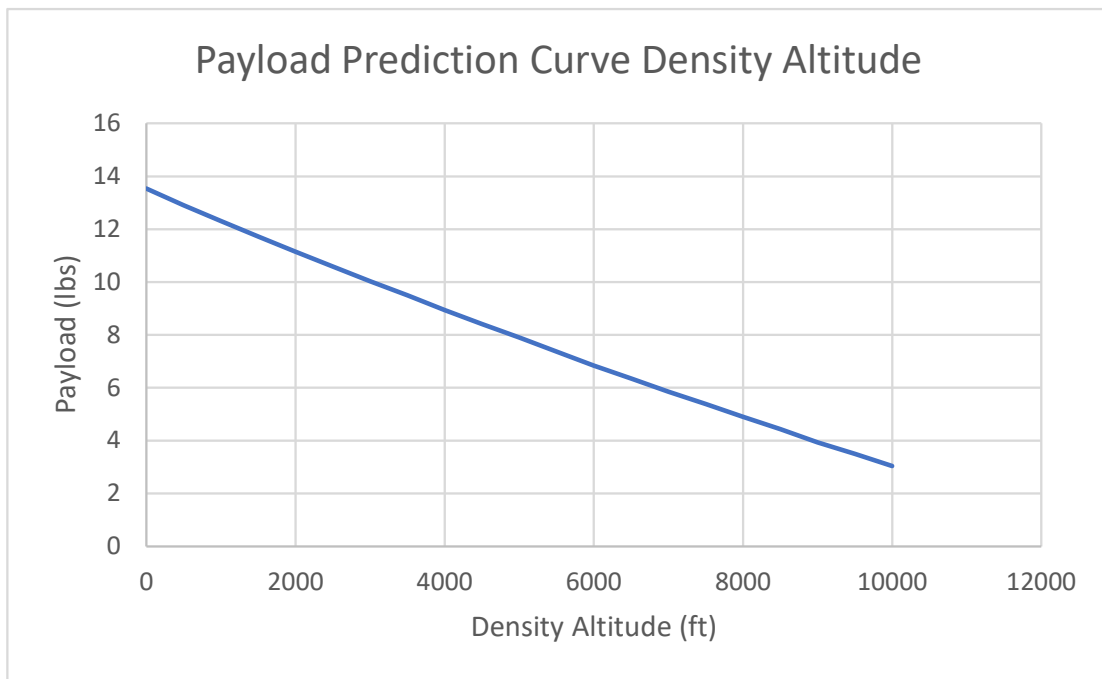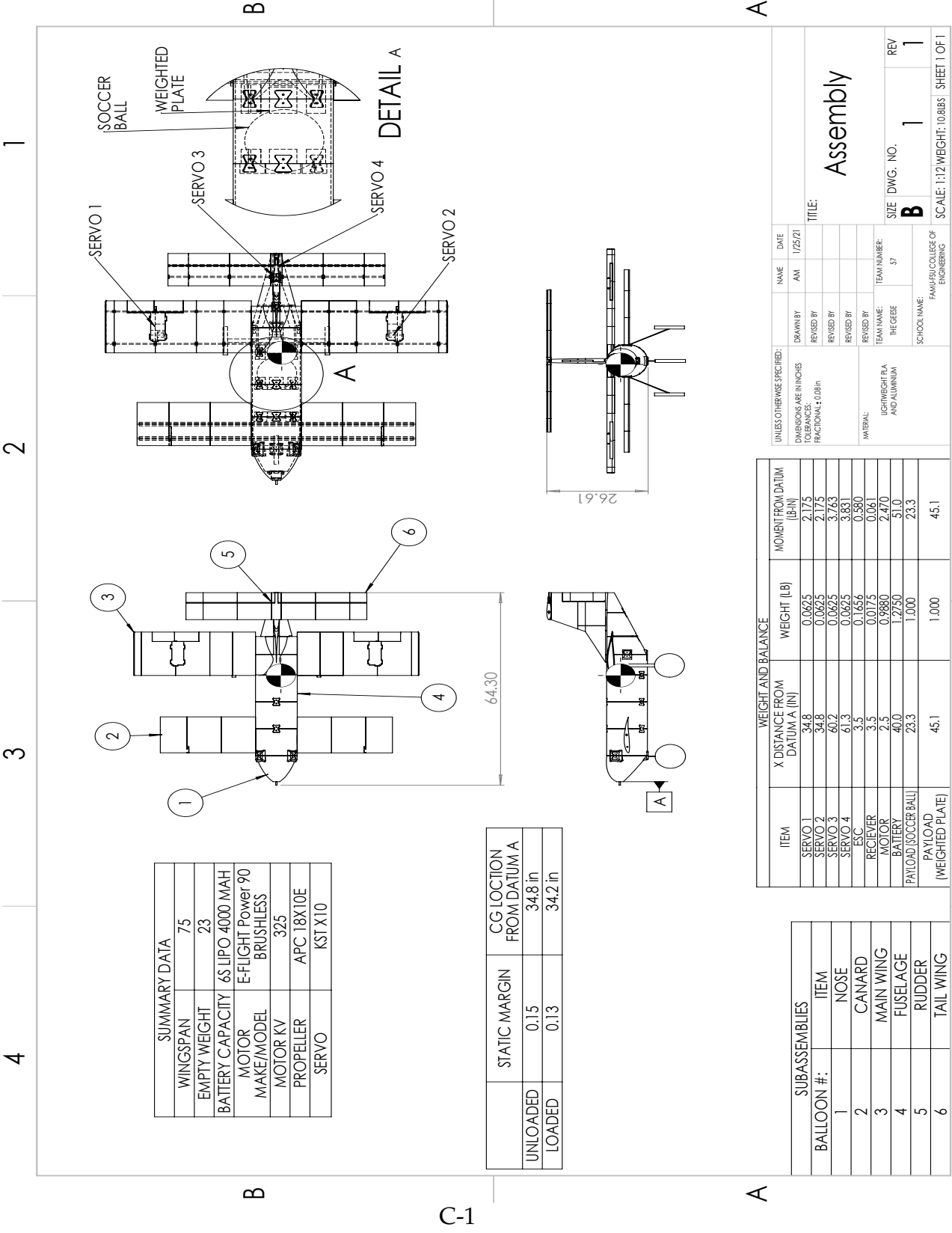

Figure B-1: Payload Prediction Plot

Plane Drawing

DETAIL A

Labels: SOCCER BALL, WEIGHTED PLATE, SERVO 1, SERVO 3, SERVO 4, SERVO 2, A

64.30

26.61

SUMMARY DATA

SUMMARY DATA	
WINGSPAN	75
EMPTY WEIGHT	23
BATTERY CAPACITY	6S LIPO 4000 MAH
MOTOR MAKE/MODEL	E-FLIGHT Power 90 BRUSHLESS
MOTOR KV	325
PROPELLER	APC 18X10E
SERVO	KST X10

	STATIC MARGIN	CG LOCTION FROM DATUM A
UNLOADED	0.15	34.8 in
LOADED	0.13	34.2 in

SUBASSEMBLIES

BALLOON #:	ITEM
1	NOSE
2	CANARD
3	MAIN WING
4	FUSELAGE
5	RUDDER
6	TAIL WING

WEIGHT AND BALANCE

ITEM	X DISTANCE FROM DATUM A (IN)	WEIGHT (LB)	MOMENT FROM DATUM (LB-IN)
SERVO 1	34.8	0.0625	2.175
SERVO 2	34.8	0.0625	2.175
SERVO 3	60.2	0.0625	3.763
SERVO 4	61.3	0.0625	3.831
ESC	3.5	0.1656	0.580
RECIEVER	3.5	0.0175	0.061
MOTOR	2.5	0.9880	2.470
BATTERY	40.0	1.2750	51.0
PAYLOAD (SOCCER BALL)	23.3	1.000	23.3
PAYLOAD (WEIGHTED PLATE)	45.1	1.000	45.1

UNLESS OTHERWISE SPECIFIED:

DIMENSIONS ARE IN INCHES
TOLERANCES:
FRACTIONAL: ± 0.08 in

	NAME	DATE
DRAWN BY	AM	1/25/21
REVISED BY		
REVISED BY		
REVISED BY		

MATERIAL:
LIGHTWEIGHT PLA AND ALUMINUM

TEAM NAME: THE GEESE

TEAM NUMBER: 57

SCHOOL NAME:
FAMU-FSU COLLEGE OF ENGINEERING

TITLE: Assembly

SIZE **B** | DWG. NO. 1 | REV 1

SCALE: 1:12 | WEIGHT: 10.8LBS | SHEET 1 OF 1

SOLIDWORKS Educational Product. For Instructional Use Only.